ROYAL SOCIETY
OF CHEMISTRY

PAPER

Check for updates

Methyl ketones: a comprehensive study of a novel biofuel†

Carolin Grütering, [ID] [ab] Christian Honecker,[c] Marius Hofmeister,[d] Marcel Neumann,[c] Lukas Raßpe-Lange,[e] Miaomiao Du,[f] Bastian Lehrheuer,[c] Maximilian von Campenhausen,[g] Franziska Schuster,[a] Maximilian Surger,[a] Birgitta E. Ebert,[h] Andreas Jupke,[g] Till Tiso, [ID] [a] Kai Leonhard, [ID] [e] Katharina Schmitz,[d] Stefan Pischinger[ci] and Lars M. Blank [ID] *[a]

For several burning reasons, humanity must rapidly reduce greenhouse gas emissions in the transportation sector. While the vision is to rely on electric vehicles in the future, the existing fleet will depend predominantly on liquid transportation fuels for the decades to come. Here, a blend of saturated and monounsaturated medium-chain length methyl ketones is suggested as a sustainable biofuel that is fully compatible with the existing diesel fleet. These methyl ketones can be produced by genetically modified *Pseudomonas taiwanensis* VLB120 at high yields from glucose. By performing a comprehensive, reductive solvent screening for *in situ* extraction of methyl ketones, a bioprocess for methyl ketone production was developed that facilitates simple product purification by decantation. The use of an advanced multiphase loop bioreactor with countercurrent liquid–liquid extraction averted stable emulsion formation in a set-up that can run in continuous mode in the future. The methyl ketones were tested extensively for their applicability in combustion engines. Here, parameters such as the derived cetane number, the flash point, and the kinematic viscosity fit into the diesel fuel specifications. Experiments in a research internal combustion engine showed that methyl ketones as a biofuel combine the efficient combustion of diesel fuel with the clean combustion of other oxygenates. Also, good storability and reduced ecotoxicology compared to common diesel fuel were demonstrated. Accordingly, the presented blend of methyl ketones can serve as an advanced drop-in fuel in the scope of the envisaged sustainable bioeconomy.

Introduction

Fossil-based transportation fuels contribute largely to global greenhouse gas emissions and accounted for about 20% in 2021.[1,2] The prospects for electric vehicles using renewable electricity are promising, offering to overcome the challenge of fossil-based transportation. However, by 2030, approximately 80% of the global vehicle fleet will still be powered by internal combustion engines.[3] These are undoubtedly far too many cars if they are running on fossil fuels as carbon neutrality should be achieved, *e.g.*, until 2050 in Europe and 2060 in China, according to the Paris Climate Agreement. In a foreseeable timeframe, liquid fuels are also necessary for long-distance and heavy-duty transportation.[4,5] Sustainably produced fuels, *i.e.*, e-fuels, biofuels, or biohybrid fuels, can profit from the current fuel infrastructure and fleet, while maintaining the beneficial high energy content of the fossil counterparts.[6–9] Industrial biotechnology has the potential to enable the transformation of traditional petroleum-based value chains to a sustainable bioeconomy relying on biomass, CO_2, green H_2, and industrial side streams as carbon sources.[10–13] Catalysts such as microorganisms can utilize these renewable, non-edible feedstocks to synthesize value-added substances such as biofuels, bioplastics, organic solvents, and biosurfactants in the declining order of the market size.[14–17]

[a]Institute of Applied Microbiology (iAMB), Aachen Biology and Biotechnology (ABBt), RWTH Aachen University, 52074 Aachen, Germany. E-mail: lars.blank@rwth-aachen.de

[b]Bioeconomy Science Center (BioSC), Forschungszentrum Jülich GmbH, 52428 Jülich, Germany

[c]Chair of Thermodynamics of Mobile Energy Conversion Systems, RWTH Aachen University, 52074 Aachen, Germany

[d]Chair and Institute for Fluid Power Drives and Systems, RWTH Aachen University, 52074 Aachen, Germany

[e]Chair and Institute of Technical Thermodynamics, RWTH Aachen University, 52062 Aachen, Germany

[f]Institute for Environmental Research, RWTH Aachen University, 52072 Aachen, Germany

[g]AVT – Fluid Process Engineering, RWTH Aachen University, 52074 Aachen, Germany

[h]Australian Institute for Bioengineering and Nanotechnology (AIBN), The University of Queensland, Brisbane, QLD 4072, Australia

[i]JARA-ENERGY, 52056 Aachen, Germany

Due to their favorable cetane numbers, medium-chain length methyl ketones gained attention as possible fuel alternatives.[18] Since the implementation of heterologous methyl ketone production in *Escherichia coli*,[19] methyl ketones have been produced in various microorganisms, including *Saccharomyces cerevisiae*, *Yarrowia lipolytica*, and *Pseudomonas putida*.[20–22] *Pseudomonas taiwanensis* VLB120 was demonstrated to be a suitable production host for methyl ketones since this strain has an exceptionally high redox cofactor regeneration rate, a trait that is beneficial for the production of such reduced products.[23] Genetic modifications for producing methyl ketones included a complete disruption of the β-oxidation cycle and the obviation of the flux from acyl-CoA esters to free fatty acids. By these means, methyl ketones were produced from glucose at 53% of the theoretical maximum yield in a fed-batch process with *n*-decane as a solvent for *in situ* product extraction, representing the highest reported methyl ketone yield so far.[24]

The addition of organic solvents to the fermentation broth for *in situ* product extraction brings a wide range of benefits to bioprocesses. These include the prevention of product degradation and evaporation, the reduction of downstream processing steps and a favorable shift of reaction equilibria.[25,26] Many applications also benefit from a reduced concentration of a toxic product in the aqueous phase and thus a better performance of the biocatalyst.[27] While a wide variety of solvents can potentially be suitable for a specific application, the applied type of organic solvent should be thoroughly investigated since the solvent is in direct contact with the fermentation broth. Inappropriate solvent choices can lead to poor phase separation or reduced biocatalyst performance among other things.[28,29] In order to systematically reduce the solution space, comprehensive solvent evaluation procedures were developed that match the requirements of biological systems. Several studies have shown that such approaches can improve the performance of bioprocesses.[30,31] For example, an extensive solvent screening was indispensable for the efficient recovery of biosurfactants by *in situ* extraction.[32] The suggested reductive, multi-step approach can serve as a blueprint for solvent selection for other applications including methyl ketone production.

However, *in situ* product extraction often goes hand in hand with the formation of stable emulsions due to surface-active compounds, such as proteins and phospholipids synthesized by the whole cell catalyst. A range of technologies were suggested to break these emulsions, including centrifugation, supercritical CO_2, and catastrophic phase inversion, besides others, however, all requiring an additional step and hence complicate purification.[33–37] Recently, a new bioreactor type, namely a multiphase loop reactor (MPLR, Fig. 1) was designed for the circumvention of cumbersome emulsion formation,[38] reducing the energy entry enormously, while compromising only little on extraction efficiency.

In this study, the previously engineered *P. taiwanensis* VLB120 (ref. 24) that efficiently converts glucose to methyl ketones was exploited, and the product mixture was evaluated as a fuel that is backward-compatible with the existing vehicle fleet. As the fermentation relies on *in situ* extraction, a hierarchical organic solvent screening was carried out, taking such
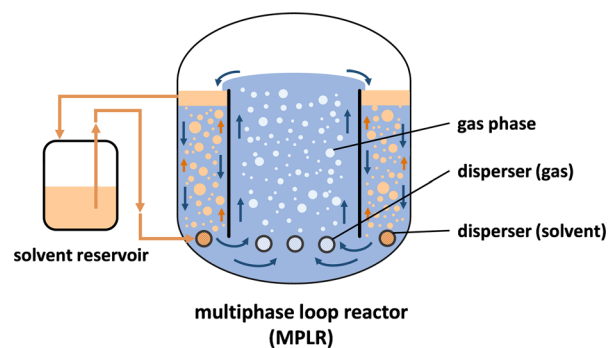

Fig. 1 Schematic representation of the multiphase loop reactor (MPLR). In the inner compartment (riser), gas spargers induce a loop flow of the aqueous phase. In the outer (downcomer) compartment, solvent dispersers are located. The solvent droplets rise and lead to continuous countercurrent liquid−liquid product extraction. In the upper part of the downcomer, a coalescing unit leads to accumulation of the solvent droplets. The organic solvent can be pumped into a solvent reservoir, from where it is continuously reintroduced into the MPLR.[38–40] MPLR = multiphase loop reactor.

different parameters as physicochemical properties, green solvent categorization, partition coefficient, biocompatibility, and suitability for extracting methyl ketones into account. 2-Undecanone was identified as a solvent with superior properties that considerably simplifies downstream processing. Under ideal conditions, as realized by the novel multiphase loop reactor, only decanting is required.[38,40,41] The resulting methyl ketone mixture was extensively evaluated for its suitability as a fuel in combustion engines based on a range of performance parameters, including flash point, viscosity, and lubrication behavior. Using this information, a surrogate mixture was assessed in terms of the combustion performance in a single-cylinder engine. The results revealed full compatibility with existing internal combustion engines and importantly superior combustion properties when compared to standard diesel fuel under the tested conditions. These positive results motivated us to investigate the ecotoxicology and the susceptibility to microbial degradation during storage. The results are discussed in the context of methyl ketones as an advanced, potentially sustainable fuel blend in existing diesel engines.

Experimental

Strains, media, and pre-culture conditions

The chemicals used in this work were obtained from Carl Roth (Carl Roth GmbH + Co. KG, Karlsruhe, Germany), Sigma-Aldrich (Merck KGaA, Burlington, USA), or TCI (Tokyo Chemical Industry Co., Ltd., Tokyo, Japan). Genetically modified *Pseudomonas taiwanensis* VLB120 Δ6 pProd was used as a methyl ketone production host.[24] The strain was maintained and cultured in the presence of 25 mg L^{-1} gentamycin and 50 mg L^{-1} kanamycin. For storage, cells were kept at −80 °C with 25 vol% glycerol in cryo stocks. All cultivation steps were performed at 30 °C. Mineral salt media (MSM, adapted from Hartmanns *et al.*, 1989 (ref. 42)) contained 2.0 g L^{-1} $(NH_4)_2SO_4$, 0.1 g L^{-1} $MgCl_2 \cdot 6H_2O$, 10.0 mg L^{-1} EDTA, 2.0 mg L^{-1}

$ZnSO_4 \cdot 7H_2O$, 1.0 mg L^{-1}, $CaCl_2 \cdot 2H_2O$, 5.0 mg L^{-1} $FeSO_4 \cdot 7H_2O$, 0.2 mg L^{-1} $Na_2MoO_4 \cdot 2H_2O$, 0.2 mg L^{-1} $CuSO_4 \cdot 5H_2O$, 0.4 mg L^{-1} $CoCl_2 \cdot 6H_2O$, 1.0 mg L^{-1} $MnCl_2 \cdot 2H_2O$, and supplemented with the respective carbon source and inducers. Additionally, in bioreactor cultivations with continuous pH regulation, 3.88 g L^{-1} of K_2HPO_4 and 1.63 g L^{-1} of NaH_2PO_4 were added, while shaken cultures had a doubled concentration of 7.76 g L^{-1} K_2HPO_4 and 3.26 g L^{-1} NaH_2PO_4 to ensure sufficient pH buffering. Optical density at a wavelength of 600 nm (OD_{600}) values for growth monitoring were determined with an Ultrospec™ 10 Cell Density Meter (Harvard Bioscience, Holliston, USA). For cultivations, the strain was streaked on a Lysogeny Broth (LB) plate with 10 g L^{-1} peptone, 5 g L^{-1} sodium chloride, 5 g L^{-1} yeast extract, and 1.5% agar (w/v). The next day, a single colony was used to inoculate 5 mL of liquid LB media without agar in a 15 mL glass tube that was cultivated at 200 rpm. The second pre-culture was performed in a 500 mL shake flask with 10% (v/v) MSM supplemented with 10 g L^{-1} glucose at 300 rpm. It was inoculated to an OD_{600} of 0.1 and cultivated until the late exponential phase for inoculation of the main culture. In main cultures in tubes, shake flasks, and bioreactors, 2 mM IPTG and 1 mM arabinose were added to the media as inducers for methyl ketone formation.

Pre-screening for physicochemical properties

An initial pre-screening of 97 potential solvent candidates was performed for the density, the log P, the melting point, and the flash point. The respective values were derived from the PubChem website, the GESTIS-Stoffdatenbank, or the website of the supplier.[43,44] 1-Octanol was included in the later screening due to its common usage for in situ extraction in bioprocesses, and nonanal was included as a negative control due to its low log P. The details of this screening step can be found in ESI file 1,† pre-screening.

Partition coefficient and interphase formation

For testing of the partition coefficient and interphase formation using the pre-selected solvents, a main culture of methyl ketone producing *P. taiwanensis* VLB120 Δ6 pProd was performed in nine 0.5 L shake flasks, each with 0.05 L of MSM with 10 g L^{-1} glucose. The initial OD_{600} was 0.1. After 52 hours at 30 °C and 300 rpm, the cultivation was stopped. 1.6 mL of the cultivation broth was shaken with 0.4 mL of the corresponding organic solvent at 900 rpm and 30 °C in a horizontal shaker in triplicates. After centrifugation of the sample for 5 min at 13 300 rpm, aqueous and organic phases were separated. For determination of the partition coefficient, the concentration of the remaining methyl ketones in the aqueous phase was measured. The partition coefficient P was calculated according to eqn (1) with c_0 and c_1 as the product concentration in the cultivation broth before (0) and after (1) the extraction, and Θ as the phase ratio (in (v/v) organic to aqueous phase) from triplicate measurements.

$$P = \frac{c_0 - c_1}{c_1 \cdot \Theta} \tag{1}$$

Interphases often occur as a third, undefined layer after phase separation for cultivation broths with in situ product extraction and lead to a loss of product and the organic solvent.[32,45] The formation of these process-hindering interphases was assessed by qualitatively analyzing pictures of the extraction vials after centrifugation.

Assessment of solvent toxicity to host

For an initial growth assay of methyl ketone producing *P. taiwanensis* VLB120 Δ6 pProd in the presence of the pre-selected solvent candidates, the main cultures were performed in closed 15 mL glass tubes using 1 mL of MSM with 2 g L^{-1} glucose and 0.5 mL of the corresponding solvent. The initial OD_{600} was 0.1. After 48 hours of incubation at 30 °C and 200 rpm, the turbidity of the aqueous phase was compared by taking pictures, since no spectrophotometric biomass measurement is possible as soon as organic solvents are present in the cultivation broth.

Shake flask cultivations with online CO_2 monitoring

For online CO_2 measurement, BlueSens BCP-CO_2 sensors connected to the BlueVis software (both BlueSens GmbH, Herten, Germany) were used. The sensors were installed on 1.3 L closed shake flasks filled with 0.05 L of MSM medium containing 3 g L^{-1} glucose and 2 mL of the respective organic solvent. The cultivations were performed at 150 rpm with an initial OD_{600} of 0.1.

Bioreactor cultivations

Stirred-tank bioreactor cultivations were performed in vessels with a total volume of 1.3 L and a working volume of 0.5 L of MSM with 2 mM isopropyl β-D-1-thiogalactopyranoside (IPTG) and 1 mM arabinose, 10 g L^{-1} of glucose, and 100 mL 2-undecanone. The cultivations were controlled by BioFlo120 units and DASware Control Software 5.3.1 (both Eppendorf SE, Hamburg, Germany). The pH was controlled at a value of 7.0 by addition of 4 M KOH and 4 M H_2SO_4 and the temperature was kept at 30 °C. The dissolved oxygen (DO) level was kept above 30% using a stirring cascade from 400 rpm to 1200 rpm. Exhaust gas analysis was performed using BlueInOne Ferm gas analyzers, and data was recorded with BlueVis (both BlueSens GmbH, Herten, Germany).

The MPLR (Fig. 1) consisted of a 5.0 L reactor glass vessel (Eppendorf SE, Hamburg, Germany) and an in-house manufactured head plate as a basis for the MPLR-specific internals. A stainless-steel cylinder separated the inner riser from the outer downcomer compartment. In the former, a 3D printed porous poly(dodecane-12-lactam) spiral sparger with a porosity of 15% and pore diameters ranging from 0.7 to 8.0 μm was used for aeration. Both riser and downcomer had probes for temperature, pH, and DO measurements. The probes in both compartments were connected to one BioFlo110 unit each (Eppendorf SE, Hamburg, Germany). The pH of the riser was kept constant at 7.0 by addition of 4 M KOH and 4 M H_2SO_4. The aeration was varied from 0.6 to 1.3 volume air per volume aqueous phase per minute (vvm) to guarantee sufficient supply

of oxygen. The aqueous phase was 4.18 L of MSM with 10 g L^{-1} of glucose. As a solvent phase, 1.0 L of 2-undecanone were pumped from the coalescing compartment to a solvent reservoir and from the solvent reservoir back to the solvent disperser in the downcomer using external peristaltic pumps. The solvent cycle consisted solely out of polytetrafluoroethylene (PTFE), stainless steel, and boron-silicate glass. Exhaust gas analysis was performed using BlueVary gas analyzers (BlueSens GmbH, Herten, Germany). For the details of the MPLR setup, refer to Campenhausen *et al.*, 2023 and ESI file 3, Fig. A.1.†[38]

Sample preparation and quantification of biological analytes

All samples from cultivations were centrifuged for 2 min at 13 300 rpm. In case of aqueous-organic two-phase cultivations, the upper, organic phase was used for methyl ketone quantification in a gas chromatography (GC, Trace GC Ultra, Thermo Scientific, Waltham, USA) equipped with a flame ionization detector (FID). 1 μL of the organic phase was injected with an injector temperature of 250 °C into a polar ZB-WAX column (30 m length, 0.25 mm inner diameter, 0.25 μm film thickness, Zebron, Phenomenex Inc., Torrance, USA) and a helium flow of 2 mL min^{-1}. An initial oven temperature of 80 °C was held for 2.5 min, then increased to 250 °C at 20 °C min^{-1} and held constant at 250 °C for 10 min. Quantification was performed using external standards quantification of 2-undecanone, 2-tridecanone, 2-pentadecanone, and 2-heptadecanone. Since no standards for the monounsaturated methyl ketones 2-tridecenone, 2-pentadecenone and 2-heptadecenone were available, their concentration was derived from their peak area using the same calibration curve as their saturated counterparts. The presence of the monounsaturated methyl ketones was confirmed using a GC with a mass spectrometer (GC-MS) as described earlier.[19,24] The aqueous phase from these aqueous-organic two-phase cultivations and centrifuged broths from cultivations without organic solvent were analyzed *via* high-pressure liquid chromatography (HPLC). After filtration through a 0.2 μm membrane filter, the metabolites were quantified in a HPLC with a refractive index and a UV detector (HPLC-UV-RI). This was performed using a DIONEX UltiMate 3000 HPLC System (Thermo Scientific, Waltham, USA) with a Metab-AAC column (300 × 7.8 mm column, ISERA). Elution was done with 5 mM H$_2$SO$_4$ at a flow rate of 0.6 mL min^{-1}, and a column temperature of 40 °C. For detection, a SHODEX RI-101 detector (Showa Denko Europe GmbH, Munich, Germany) and a DIONEX UltiMate 3000 Variable Wavelength Detector set to 210 nm were used. The substrates were identified and quantified *via* retention time and UV/RI quotient compared to corresponding external standards, respectively.

Fluid mechanical properties

Kinematic viscosity. All fluid mechanical measurements and fuel property measurements were performed with a surrogate mixture of the saturated methyl ketones (22.4 vol% 2-undecanone, 51.2 vol% 2-tridecanone, and 26.4 vol% 2-pentadecanone) representing the chain length distribution that was

determined for methyl ketones produced by *P. taiwanensis* VLB120.[24]

The kinematic viscosity of the sample liquid was determined by means of an Ubbelohde viscometer according to DIN 51562.[46] For the temperature control of sample liquid and viscometer a temperature control unit with a manufacturer guaranteed accuracy of 0.01 K was used. To ensure a constant and uniform temperature distribution, the viscometer was placed in the temperature control unit for 30 min before each measurement series. The actual measurement series consisted of two preliminary measurements and five main measurements where only the main measurements are considered for the evaluation of the viscosity results.

$$\rho_L = \frac{m_{buoyancy} - m_{measured}}{V_{buoyancy}} \quad (2)$$

Density. For the measurement of liquid density, a setup shown in ESI file 3, Fig. A.2† was used. Essentially, the setup consists of a tension scale with a measurement resolution of 0.01 mg, a buoyancy body, and a vessel filled with the sample liquid. According to the Archimedes' principle, the liquid density ρ_L equals the difference between measured mass $m_{measured}$ and the actual mass of the buoyancy body $m_{buoyancy}$ divided by the volume $V_{buoyancy}$ of the buoyancy body (eqn (2)).[47] The described measurement procedure was performed ten times for each measurement series.

The temperature of the sample liquid was controlled by means of an external tempering unit and an internal heat exchanger. The temperature accuracy of the used tempering unit is 0.02 K.

Surface tension. For the determination of the surface tension the du Noüy ring method according to DIN EN 14370 was used.[48] For the evaluation of the results, the mean value of five single measurements was used. As with density, a combination of external temperature control unit and internal heat exchanger was used to control the temperature of the liquid. The temperature accuracy of the used tempering system was 0.02 K.

Material compatibility. For the evaluation of material compatibility of the methyl ketone blend, immersion tests according to DIN ISO 1817 and high frequency reciprocating rig (HFRR) measurements were conducted.[49] While the insertion tests provide information on the compatibility of potential sealing materials and the fuel, the HFRR test determines the lubricity of the fuel according to ISO 12156.[50]

Immersion test. To evaluate the material compatibility of the methyl ketone blend and different sealing materials an immersion test according to DIN ISO 1817 was conducted. During the test, reference sealing specimens according to ISO 13226 were immersed into the sample liquid for a total duration of 672 h.[50] At defined times, the specimens were removed from the sample liquid and measured regarding the change of volume, mass, and hardness. The international rubber hardness degree is determined according to DIN ISO 48. For each elastomer specimen, six measurements were conducted, with a duration of each measurement of 30 seconds.[51]

For the volume measurement, the same setup as for the determination of the liquid density, namely ESI file 3, Fig. A.2† was used. In contrast to the density measurement, the density of the liquid ρ_L is known, so that the volume of the specimen $V_{specimen}$ can be calculated using eqn (3).

$$V_{specimen} = \frac{m_{buoyancy} - m_{measured}}{\rho_L} \quad (3)$$

The mass of the elastomer specimen was measured by means of a precision scale with a resolution of 0.01 mg and a device-specific standard deviation of 0.02 mg. Volume and mass measurement were repeated three times for each specimen and the corresponding mean value was calculated. Three test specimens were tested for each combination of sealing material and sample liquid. The geometric dimensions of the sealing specimens were $25 \times 25 \times 2$ mm^3 and the volume of the sample liquid was 40 mL. During the entire test period, the specimens and liquid samples were kept inside a climatic chamber with a temporal and local temperature accuracy of 0.5 K at 23 °C.

High frequency reciprocating rig (HFRR) test. The HFRR test according to ISO12156 evaluates whether a fuel has good lubricating properties. For this purpose, a steel ball was pressed onto a steel surface and moved back and forth. Subsequently, the resulting wear area was measured by means of a digital microscope, with a translational resolution in the x and y axis of 350 nm. The average value of the width and length of the wear area is defined as the wear scar diameter (WSD). Small values for the WSD are associated with good lubricating properties. The described measurement process was repeated five times for each sample liquid. The test duration was 75 min and the liquid temperature 60 °C.

Flash point and boiling point prediction

To complement experimental data, flash points and boiling points were predicted with computer-aided methods. Predictions for both properties were performed using the Conductor-like Screening Model for Real Solvents (COSMO-RS).[52,53] The COSMO-RS model in combination with density functional theory calculations allows the prediction of multiple thermodynamic properties based on the molecules' 3D structure. The molecular geometries were optimized in an implicit solvation model assuming an ideal conductor. The screening charge densities of the molecules in a self-consistent state (COSMO-state) were obtained, which, when transformed into a histogram, yielded the sigma profiles that were the basis for all mixture and pure component properties calculated with the COSMO-RS model.[52] The density functional theory calculations are performed using the BP-86 functional and a def2-TZVPD basis set.[54–56] Geometry optimization and conformer search were executed in the COSMOconf Software while property data was predicted using the COSMOthermX19 Software package (both Dassault Systèmes, Vélizy-Villacoublay, France).

Determination of the derived cetane number

The derived cetane number (DCN) is a measure of the ignitability of a diesel fuel and thus a central aspect of the fuel's suitability in combustion engines. For the methyl ketone blend (22.4 vol% 2-undecanone, 51.2 vol% 2-tridecanone, and 26.4 vol% 2-pentadecanone), the DCN was determined in an AFIDA 2085 advanced fuel ignition delay analyzer (ASG Analytik-Service AG, Neusäß, Germany). This device uses a heated and pressurized constant volume combustion chamber of 0.39 L to measure ignition delay times.[57] For injection, the fuel candidate was pressurized up to 1200 bar, and the constant-volume combustion chamber reached 50 bar and 730 °C using compressed air. Ignition was detected by a defined relative pressure rise, measured through a dynamic pressure transmitter. From these ignition delay times, the DCN was calculated based on a calibration curve of reference fuels in accordance with ASTM D8183.[58]

Combustion properties in a single-cylinder research engine

Engine experiments were conducted using a single-cylinder research engine designed to mimic the characteristics of contemporary light-duty compression ignition engines. The engine has a bore of 75 mm and 0.39 L of displacement. The engine setup was described earlier in detail.[59–61] To achieve realistic conditions that are challenging regarding the trade-off of NO$_x$ and soot, a compression ratio of 19 : 1 was chosen for this test.

Boost pressure (p_{in}), exhaust pressure (p_{ex}), and charge air temperature (T_{in}) were externally conditioned to the desired value. Exhaust gas recirculation (EGR) was performed by cooled high-pressure EGR. Oil and coolant were externally conditioned to 90 °C. The engine speed (n) was controlled using an eddy current dynamometer and an external electric motor to enable operation also at very low load. An automatic controller adjusted the centre of combustion (CA50) and the indicated mean effective pressure (IMEP) to the desired target value by adapting the main injection duration of injection (DOI) and start of injection (SOI). Indication data was obtained via a Kistler 6041A water-cooled piezoelectric pressure transducer (Kistler Instrumente AG, Winterthur, Switzerland) and analyzed using the FEVIS combustion analysis software (FEV Software and Testing Solutions GmbH, Aachen, Germany) in real-time.

Relevant engine operating points were chosen based on New European Driving Cycle and Worldwide Harmonized Light Vehicles Test Cycle reference points calculated for a 1590 kg passenger car with a 1.6 L diesel engine.[59,60] Additionally, a comparison point for alternative combustion systems was added to the test matrix.[62] All tested operating points were optimized for diesel operation, yielding standard values for CA50 rail pressure (p_{rail}), p_{in}, p_{ex} as well as pilot-injection offset (t_{pi}), and DOI, when applicable.[60,62] These parameters were kept constant between fuels. All measurements were conducted under stationary operation, granting sufficient time for the system to stabilize prior to measurement. Soot was measured three times and averaged, indication data was cycle-averaged over 50 consecutive cycles, and the remaining data was sampled in 10 Hz intervals and averaged for 30 seconds to ensure statistical validity. The tests were carried out as EGR variations with constant p$_{in}$, beginning with fresh air. To

determine the suitability of the methyl ketone blend from an emission perspective, a FEVER exhaust analysis system (FEV Software and Testing Solutions GmbH, Aachen, Germany) was used to measure unburned hydrocarbons (HC), CO, CO_2, residual O_2, NO_x, and NO. Soot was measured with the filter paper method using an AVL415 SmokeMeter (AVL List GmbH, Graz, Austria). The intake CO_2 concentration was used to determine EGR rates.

Storability test of 2-undecanone

As a representative of the methyl ketones, 2-undecanone was compared to summer diesel and winter diesel. Each fuel was supplemented with 4% (v/v) rape seed methyl ester in triplicates. To mimic the biological origin of the methyl ketone, 2-undecanone was mixed with media supernatant. This supernatant was generated from a main culture of *P. taiwanensis* VLB120 Δ6 prod in 500 mL shake flasks with 50 mL of MSM with 10 g L^{-1} of glucose and arabinose and IPTG for methyl ketone formation. After 48 hours of cultivation, the broth was centrifuged for 20 min at 12 000 rpm and stored at −20 °C until further usage. After 30 seconds of mixing this supernatant with 2-undecanone, the methyl ketone was separated from the cultivation broth by settling for 24 hours. The storability experiments were performed in a closed 500 mL flask, with 50 mL of aqueous phase (0.1% NaCl) and 250 mL of the corresponding organic phase, resulting in 200 mL headspace. The bottle was not shaken and kept in the dark to mimic a storage tank. Valves between the opening of the bottle and the BCP-CO_2 sensor (BlueSens GmbH, Herten, Germany) enabled relocation of the sensors between the flasks. The water phase was inoculated with a mixture of 20 microbes as specified by Leuchtle *et al.*, 2018.[63] Pre-cultures of these microorganisms were prepared at 30 °C and 200 rpm in LB medium, yeast extract peptone medium, potato extract glucose bouillon (26.5 g L^{-1}), and malt extract medium for bacteria, yeasts, *Rhodotorula mucilaginosa*, and molds, respectively. The method was adapted according to Ackermann *et al.*, 2021 for methyl ketones.[64] ESI file 3, Table A.1† shows the defined inoculum used for the assessment of storability.

Ecotoxicology assessments

The acute toxicity of methyl ketone blends A and B was tested by performing zebrafish (*Danio rerio*) fish embryo toxicity tests. Blend A was a mixture of the saturated methyl ketones with 22.4 vol% 2-undecanone, 51.2 vol% 2-tridecanone, and 26.4 vol% 2-pentadecanone. Blend B was derived from cultivation broth with the unsaturated methyl ketones, namely 2-undecanone, 2-tridecanone, 2-tridecenone, 2-pentadecanone, 2-pentadecenone, and 2-heptadecenone. The detailed method of the toxicity test has been described previously.[65] Briefly, zebrafish embryos were exposed to two different mixtures of methyl ketones for 96 hours. Fertilized zebrafish eggs were examined under the microscope, then those developed normally were transferred into glass vials filled with exposure solutions (one egg per vial with 11 mL exposure solution). Each exposure concentration and control group consisted of ten glass

vials with eggs. The testing concentration ranged for mixture A and mixture B were 0.10 to 2.00 mg L^{-1} and 1.00 mg L^{-1} to 3.00 mg L^{-1}, respectively. Ethanol (concentration: 800 μL L^{-1}) was added as a co-solvent in both exposure group and negative control group, to enhance the solubility of methyl ketones in water. All zebrafish embryos were incubated at 26 °C and a 14 : 10 hour light : dark cycle. All the embryos were examined under the microscope every 24 hours, and abnormal development, lethality as well as the number of hatched embryos were recorded. The median effective concentration (EC_{50}), 50% lethal concentration (LC_{50}), lowest observed effect concentration (LOEC), and no observed effect concentration (NOEC) were calculated by using the software ToxRat Professional (ToxRat Solutions GmbH, Alsdorf, Germany).

Results and discussion

Solvent screening

Physicochemical parameters. A high number of organic solvents is potentially suitable for efficient, sustainable, and safe *in situ* extraction of methyl ketones. In order to systematically reduce the initial number of candidates, 97 organic solvents were evaluated regarding density, log P, melting point, and flash point (Table 1, ESI file 1†). The density of a solvent is of relevance because of the suitability for gravity-based separation techniques. The threshold was set to 880 kg m^{-3} to ensure a sufficient density difference to the aqueous fermentation that has a density of approximately 1000 kg m^{-3}. The log P as a measure of the hydrophobicity of a liquid describes the miscibility with the fermentation broth and can also serve as a first hint for estimating the compatibility of the solvent with the microbial production host. With a restriction to solvents with a log P higher than 3.4, the respective solvent candidate is hydrophobic enough to avoid adverse cross solubility with the cultivation broth as well as interaction with the cell membrane of the production host.[66,67] With a melting point lower than 18 °C, the liquid state of the candidate at cultivation conditions is ensured. The threshold for the flash point was set to values higher than 40 °C to exclude solvents that are unsafe due to flammability. The described approach reduced the initial 97 solvents to a set of 22 solvents.

Weighted decision matrix. The next factors that were considered for the solvent selection were the toxicity on the production host, the green solvent score, the partition coefficient of the methyl ketones, and the formation of interphases.

As a first measure of solvent toxicity on the production host, the microbe was grown in the presence of 33 vol% of the

Table 1 Physical parameters and respective limits for reduction of solvent candidates

Factor	Limit	Unit
Density	<880	kg m^{-3}
Log P	≥3.4	—
Melting point	<18	°C
Flash point	>40	°C

respective solvent in a growth assay. After 48 hours of incubation time, cell growth was compared by estimating the turbidity of the aqueous phase (ESI file 2†). As suggested by Prat *et al.*, 2016 the candidates were also examined regarding health and safety scores.[68] The partition of the methyl ketones between the aqueous cultivation broth and the organic solvent after extraction is one of the major requirements for the *in situ* extraction. All solvent candidates show high partition coefficients of at least 24 for ethyl oleate and up to 135 for ethyl laurate (Fig. 2).

Lastly, interphase formation was compared as a measure of efficient and reproducible separation of the aqueous and organic phase after the extraction. In order to systematically compare and rank 22 solvent candidates regarding these properties, a weighted decision matrix was created. For this, each property was given a weight regarding its importance for the biotechnological synthesis setup. Since the growth of the production host in the presence of the solvent is fundamental, this factor was given the highest weight of 40%. The green solvent score had a weight of 30%, the interphase formation and partition coefficient accounted for 20% and 10%, respectively. Then, all solvents were graded considering all properties with grades from one (worst performance) to five (best performance). A detailed explanation for the ranking including all results is given in ESI file 2.† To generate a solvent score by which the candidates could be ranked, the sum of the weighting times the score was calculated.[69] This gave each solvent a specific value for direct comparison. Using the solvent score, all tested candidates could be ranked according to their performance, with octyl octanoate as the highest scoring solvent and nonanal with the lowest score. Octyl octanoate, farnesene, methyl decanoate, 2-undecanone, hexadecane, and ethyl decanoate had a score equal to or higher than 92% of the theoretical maximum score, so these were considered in the subsequent step of the solvent screening.

Biocompatibility. For a suitable solvent candidate, the growth behavior of the cells in the presence of the organic phase is an essential information. Therefore, biocompatibility and biodegradation of octyl octanoate, farnesene, methyl decanoate, 2-undecanone, hexadecane, and ethyl decanoate was assessed
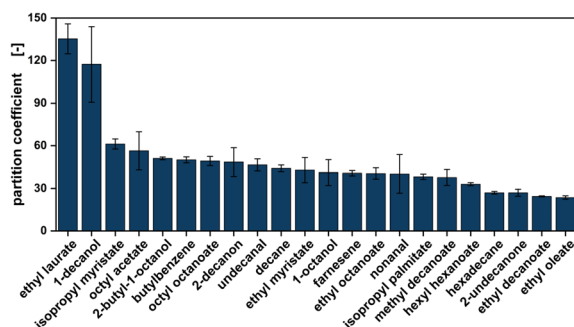
Fig. 3 Biocompatibility and biodegradability assessment of the solvents. CO_2 accumulation in the headspace of closed shake flasks in the presence of pre-selected solvent candidates. To ensure comparability of the course of the graphs, the data was standardized for the same vol% CO_2 at the point of reaching the stationary phase. The data are shown as mean values with standard deviation (shaded area) of biological duplicates.

in shake flask cultivation by online monitoring of the CO_2 accumulation in the headspace (Fig. 3) in the presence of the corresponding solvent.

The production host was able to grow in the presence of all pre-selected solvents. The highest growth rates were measured with 2-undecanone and ethyl decanoate. Especially in the first hours, the production host grew best with 2-undecanone.

In the presence of farnesene, a reduced growth rate was measured. Additionally, with octyl octanoate and methyl decanoate, a second increase in the CO_2 signal was observed, indicating biodegradation of the solvent. Thus, the production host was shown to use these solvents as a carbon source, which impairs the envisaged recycling of the solvent.

Accordingly, both delayed and decelerated growth on glucose and usage of the solvent as a carbon source is unfavorable for the pursued methyl ketone production process. 2-Undecanone proved to be a candidate that neither caused a delay of the primary growth phase nor was degraded by the microorganism.

2-Undecanone as a solvent for *in situ* extraction of methyl ketones in bioreactors

With the described solvent screening procedure, 2-undecanone was found as a suitable solvent candidate regarding physicochemical parameters, growth assays, partition coefficient, interphase formation, biocompatibility, and biodegradability. Notably, it also ranks among the best solvents regarding its properties in health and safety assessments, which reduces the risks for the operators. Furthermore, this C_{11} methyl ketone is one of the product congeners itself. Apart from the advantages of 2-undecanone mentioned above, it also holds the big advantage of a decisively simplified product purification. For recovery of the methyl ketone mixture, no costly or energy demanding techniques for solvent removal such as distillation

Fig. 2 Partition coefficients of the methyl ketones in solvent candidates and fermentation broth. The coefficients represent methyl ketone extraction from the aqueous cultivation broth using 22 solvent candidates. The obtained values were included in the ranking for the weighted decision matrix. The data are shown as mean values with standard deviation of triplicate measurements.
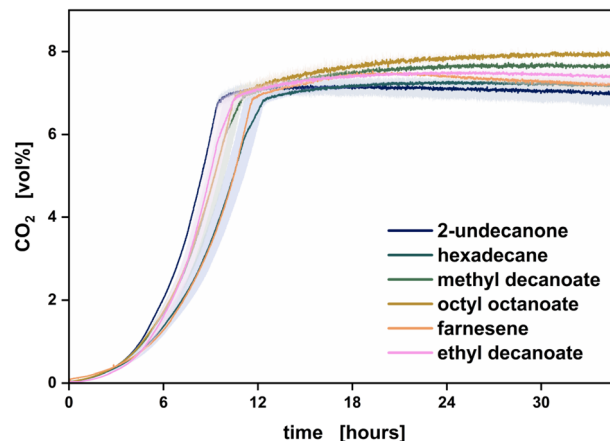
must be applied. The organic phase from the bioprocess can be used directly as the final product, for example as a biofuel blend. It was shown for other bioprocesses with *in situ* product extraction that a solvent that is compatible with the final product formulation can significantly lower production costs and minimize environmental impacts. This is especially true for bulk products like biofuels.[70,71] Additionally, 2-undecanone has a log *P* of 4.1. This is in the lower range of the log *P* values that most microorganisms can tolerate for growth.[66] Since the production host has a high tolerance to this solvent, 2-undecanone can contribute to autosterile conditions in the envisaged bioprocess. Accordingly, the performance of 2-undecanone as a second liquid phase was tested in a stirred tank bioreactor (Fig. 4A). The cultivation revealed superior suitability of 2-undecanone for continuous *in situ* extraction of methyl ketones. During the batch phase, there was no foam formation as previously observed during *in situ* extraction of methyl ketones with *n*-decane.[19,72,73] However, emulsion formation still happened in the stirred tank bioreactor (STR)

Fig. 4 Methyl ketone production with 2-undecanone as the organic phase for *in situ* extraction in a stirred tank bioreactor (STR, A) and a novel multiphase loop reactor for improved phase separation (MPLR, B). A schematic representation of the MPLR can be found in Fig. 1, and pictures of the cultivation broth of both A and B can be found in ESI file 3, Fig. A.1.† The OD_{600} value as a measure for biomass concentration could only be measured for the cultivation in the MPLR, since here no emulsification occurred that usually hinders measurement of the OD_{600}. Note that only one set of OTR data is shown in A and B. OTR = oxygen transfer rate. The data in A are shown as mean values with standard deviation of biological triplicates.

and the organic and the aqueous phase had to be separated by centrifugation (ESI file 3, Fig. A.1†). To circumvent this, the STR-based bioprocess was transferred to the multiphase loop reactor (MPLR, Fig. 4B), where aeration happens in the inner compartment (riser), and the methyl ketones are extracted by countercurrent liquid–liquid extraction in the outer compartment (downcomer). Because there were no peaks in shear stress due to stirring, highly reduced emulsification occurred compared to the STRs.[38] Stable phase separation was achieved in the coalescing unit. From here, a coherent layer of the organic phase formed, which was then continuously recirculated. Pictures of the cultivation broth corresponding to Fig. 4A and B are shown in ESI file 3, Fig. A.1.† It should be noted that no biological replicates could be performed for the cultivation in the MPLR, since only one version of this unique bioreactor setup was available. However, the cultivation ran stable and showcases the potential of the MPLR.

Notably, the product yield of both STR and MPLR was similar (44 $mg_{methyl\ ketones}\ g_{glucose}^{-1}$ for the MPLR and 50 $mg_{methyl\ ketones}\ g_{glucose}^{-1}$ for the STR), while detrimental formation of stable emulsions was circumvented in the latter. Also, oxygen supply was always sufficient for non-oxygen limited growth and product formation. This proof-of-concept cultivation showed that by using 2-undecanone for *in situ* extraction in the MPLR, phase separation can be achieved by settling. Here, the vision is to run the MPLR in continuous mode, where the production host would continuously produce the organic phase for product extraction. Accordingly, 2-undecanone also fits into the envisaged solvent recycling in this bioprocess. To assess the applicability of the methyl ketone blend as a biofuel, a proxy blend of methyl ketones representing the produced congener chain length distribution[74] was subjected to different experiments.

Fuel properties of the methyl ketone blend

Next, the fuel properties and the material compatibility of the methyl ketone blend were determined. Table 2 shows the determined values of the methyl ketones and the corresponding values of fossil diesel. The DCN of 64 is substantially higher than the DCN required by EN590 and higher than the DCN of the currently used diesel. The flash point, the kinematic viscosity, and the lubricity fulfil the requirements of EN590.

The density at 15 °C could not be determined since the mixture forms crystals at 17 °C. However, at 20 °C, the density fits into the requirements of the norm. Consequently, the density criterion can only be fulfilled by adding additives such as 1-octanol for lowering the freezing point.

The immersion test for material compatibility was performed according to DIN ISO 1817 (Fig. 5). Only for diesel and DnBE (di-*n*-butyl ether) results within the tolerance area for static or dynamic seals can be achieved. For most of the investigated bio-hybrid fuels, the change of hardness as well as volume change exceed the tolerance range. This also applies for the methyl ketone blend indicated by the green marker.

Therefore, the methyl ketone blend is not compatible with common elastomer materials and would most likely lead to failure in a technical real-life application. The highest value for
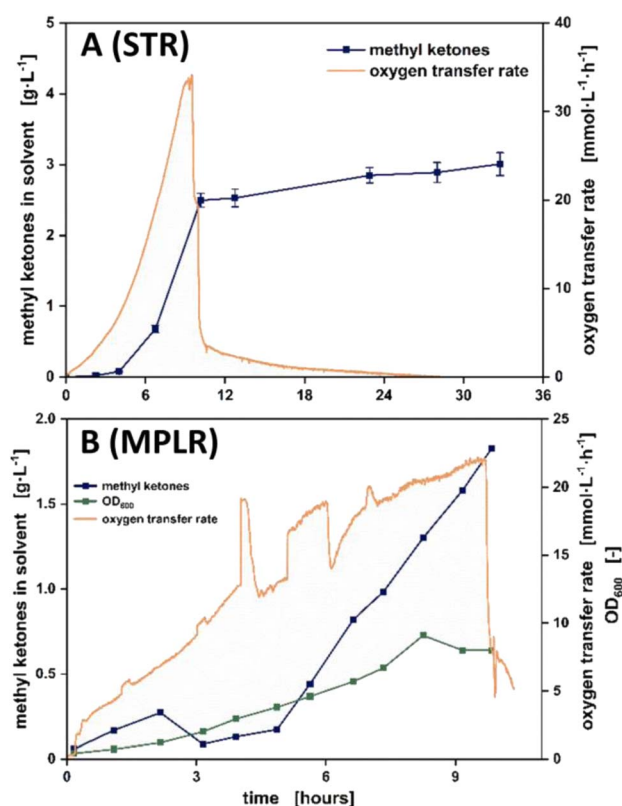
Table 2 Selected properties of fossil diesel and measured and simulated properties of the methyl ketone blend (22.4 wt% 2-undecanone, 51.2 wt% 2-tridecanone, 26.4 wt% 2-pentadecanone) and the specifications according to the EN590 norm

	Unit	EN 590 norm	Fossil diesel[75]	Methyl ketones
Molecular weight	g mol^{-1}	—	~200	210.1
Derived cetane number	—	>51	55	64[a]
Flash point	°C	>55	67	115.6[b]
Boiling point	°C	—	180–360	268[b]
Kinematic viscosity at 40 °C	mm^2 s^{-1}	2.0–4.5	~2.6	2.4
Density at 15 °C	kg m^{-3}	820–845	835	833.1[d]
Lubricity, wsd	μm	<460	301–544[76]	300[c]
Oxygen mass fraction	—	—	—	8.1
Hydrogen mass fraction	—	—	—	13.1
Carbon mass fraction	—	—	—	78.8
Lower heating value	MJ kg^{-1}	—	35.7	39.1

[a] Derived cetane number determined in the AFIDA. [b] Flash point, vapor pressure, and boiling point determined by simulations in COSMO RS. [c] Kinematic viscosity and wsd measured according to DIN 51562 and ISO12156. [d] Density of the methyl ketone blend measured at 20 °C. wsd = wear scar diameter; AFIDA = advanced fuel ignition delay analyzer.
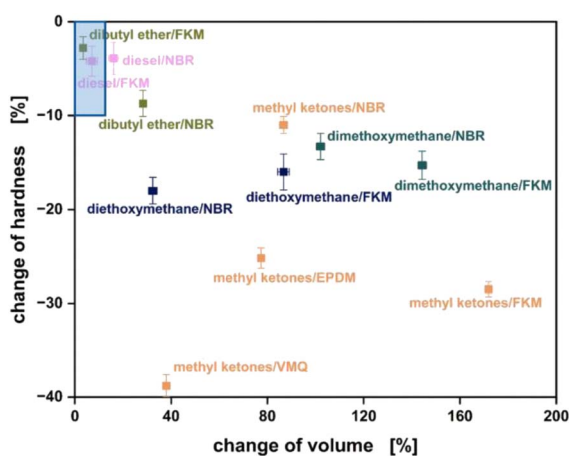
Fig. 5 Change of volume and hardness for different bio-hybrid fuels and reference elastomer sealing materials. Light blue area shows the tolerance area for dynamic seals. FKM = fluorine kautschuk material; NBR = nitrile butadiene rubber; EPDM = ethylene propylene diene monomer rubber; VMQ = vinyl methyl silicone. The data are shown as mean values with standard deviations of six replicate measurements.

volume change is 172% and is obtained for fluorine kautschuk material (FKM). The most significant decrease in hardness of −39% is observed for vinyl methyl silicone (VQM). The immersion test was also conducted for different thermoplastic sealing materials. Since the investigated thermoplastic materials are not available as reference materials, technical sealings were used.[47] For all investigated thermoplastic materials, no significant change in the sealing properties was observed. The change for all investigated parameters was less than 0.25% and is within the measurement accuracy of the used methods. The investigated methyl ketone blend fits into the standards defined by EN590 with some minor adaptions. The high DCN of the methyl ketone blend is especially beneficial for the envisaged application in combustion engines. Additionally, the WSD values for lubricity are low compared to other fuels, which is favourable in terms of friction and wear.

However, the pure methyl ketone blend would not perform well in real-life applications regarding compatibility with the materials present in the fuel segment of vehicles.

The materials were co-evolved to be compatible with the historically present fuels, namely diesel and gasoline. Thus, adaptions with regard to the sealings to PTFE would be necessary in order to use methyl ketones as a fuel.[47]

Combustion behavior in a single-cylinder research engine

To assess the suitability of the methyl ketone blend under realistic conditions, engine testing in a single-cylinder research engine was performed on an operating range covering six representative speed-load points ranging from low load to medium part-load. Fig. 6 shows an overview of the typical load point in the urban driving range. The combustion behavior of the methyl ketone blend is characterized by a short ignition delay and low pressure rise rates (PRR), which are essential for smooth engine operation. At high, usually challenging EGR rates, combustion showed a high share of mixing controlled combustion. This can be attributed to the high reactivity of the methyl ketones, as evidenced by the high DCN of 64.

The resulting relatively short ignition delay times (6.84 degree crack angle (°CA) in the non-EGR point shown here instead of 7.25 °CA for diesel) are critical in maintaining low noise and good combustion efficiency. Simultaneously, the use of methyl ketones brought about a significant reduction in soot emissions due to the presence of molecular oxygen in the fuel. Notably, this reduction did not compromise engine noise or efficiency characteristics by virtue of avoiding the shift towards a more premixed combustion that is commonly observed for alternative diesel fuels such as 1-octanol.[60,61,77,78] Maintaining a high share of diffusive combustion also averted the formation of overly lean areas in the fuel spray, thus allowing for low HC and CO emissions. Those were slightly better than for diesel combustion.

Especially in the lower load points, a considerable efficiency benefit could be discerned when using the methyl ketone blend, aided by comparably complete combustion. Towards higher

Fig. 6 Efficiency and emission results for a selected lower part load operating point, comparing the methyl ketone blend with diesel. $N = 1500$ min^{-1}; IMEP = 6.8 bar; $p_{rail} = 900$ bar; CA50 = 5.8 °C AaTDC; $p_{in} = 1.5$ bar; $p_{exh} = 1.6$ bar. η = indicated efficiency; FSN = filter smoke number; SOI = start of injection; DOI = duration of injection; PRR = pressure rise rate; HC = unburned hydrocarbon; λ = relative air fuel ratio; EGR = exhaust gas recirculation; IMEP = indicated mean effective pressure; °CAaTDC = degree crank angle after top dead center. All measurements were performed under stationary conditions. Soot was measured in triplicates and averaged, indication data was cycle-averaged over 50 consecutive cycles, and the remaining data was sampled in 10 Hz intervals and averaged for 30 seconds to ensure statistical validity.

loads, some increase in premixing may have been beneficial to shorten combustion durations.

Soot emissions are considerably reduced compared to the diesel baseline, which would, in a real-life use case, translate to a reduced need for diesel particulate filter regeneration, thus lowering fuel consumption and wear on engine, oil, and after-treatment system along with effectively further reduced tailpipe emissions. From an aftertreatment point of view, the slightly lower exhaust gas temperature (T_{exh}) might lead to difficulty maintaining or reaching the minimum temperature for catalyst activity and may require further, more specific, investigations during vehicle approval.

The benefits of the methyl ketone blend were found to be more pronounced in the lower loads and slight efficiency drawbacks appeared in higher loads. The data for the conditions before EGR-addition and for operation with very high levels of EGR to achieve a Euro6 NO$_x$-level[60] show that both diesel and the methyl ketone blend burn highly diffusive even

under adverse conditions, indicated by the cumulative normalized heat release (ESI file 3, Fig. A.3†). For very high EGR-levels, the methyl ketone blend is effectively burning slightly earlier than diesel, as the high DCN leads to slightly shorter ignition delay and high EGR-tolerance, while the mixing-controlled combustion leads to both reaching CA50 simultaneously. Under these conditions, diesel combustion is already drifting away from its desired behavior as the share of premixed combustion rises. While this limits the soot emissions at that point to still barely acceptable levels, the combustion noise for diesel is severely elevated. Avoiding this shift in combustion mode is thus advantageous and in fact also commonly observed with EN1594 fuels.[78,79]

Thus, applied to an unmodified diesel engine, it is likely that no control adaptations would be required to maintain emission compliance, thereby enabling the use of this methyl ketone blend as a drop-in fuel with no need for modifications from a combustion point of view. In addition, their improved EGR compatibility grants this methyl ketone blend the potential to further lower emissions by increasing EGR rates of either adapted or dedicated engines or as pilot-ignition fuel.

Microbial storage stability

With these favourable results in hand, the storage ability and ecotoxicology of the methyl ketones was assessed. To test the storability of methyl ketones as a fuel candidate, CO_2 formation in the presence of 2-undecanone as a representative of the methyl ketones was measured in simulated oil tanks and compared to summer and winter diesel (Fig. 7). CO_2 as the endpoint of metabolic activity serves as a marker for microbial activity.[80] Detailed information about the used microorganisms and storage conditions can be found in ESI file 3, Table A.1.† Until day eight, the simulated storage tank with methyl ketones
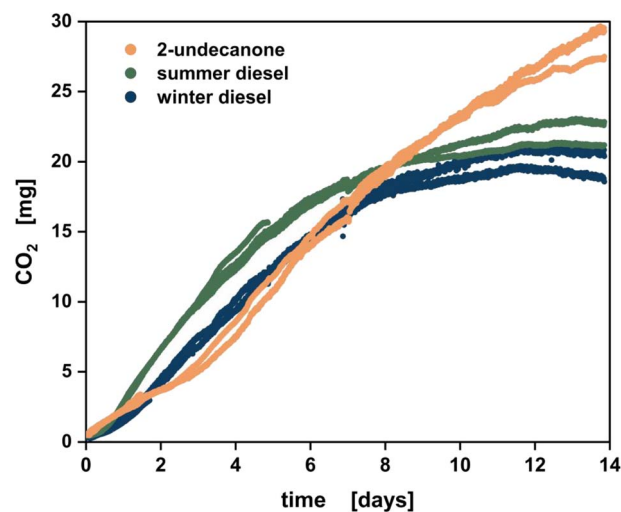

Fig. 7 Investigating fuel storage in the presence of microbial contaminations. CO_2 formation was used as a sign for microbial activity in the presence of 2-undecanone, a representative of the methyl ketones, summer diesel, and winter diesel in simulated storage tanks. The data are shown as biological triplicates.

showed a comparable CO_2 formation to winter diesel and a lower CO_2 formation than summer diesel. During the 14 day assessment period, around 30% more CO_2 was formed in the presence of methyl ketones compared to the diesel variants. After the assessed 14 days, the CO_2 level of the diesel variants stabilized, while the curve with the methyl ketones was still increasing. Hence, in short storage, methyl ketones have a similar storability to winter diesel, which is more stable against microbial degradation than summer diesel due to additives for decreasing the melting point.[81,82] In longer storage experiments, methyl ketones have a reduced storability compared to diesel. This is probably due to the keto group at the C_2 position of the methyl ketones, which can serve as a starting point for enzymatic degradation. In contrast, diesel consists mostly of saturated hydrocarbons.[83–86] Also, the methyl ketones were mixed with cultivation broth of *P. taiwanensis* VLB120 Δ6 pProd prior to this storability test to simulate its biological origin. This way, potential nitrogen and phosphorus sources can be present in the methyl ketones, that help to promote growth of microorganisms.[87] Fermentation broth carry over can be strongly reduced in an industrial production plant.

Ecotoxicological assessment of the methyl ketone blend

The acute toxicity of two blends of medium-chain length methyl ketones was assessed by performing a fish embryo toxicity test with zebrafish embryos (*Danio rerio*). Blend A contained the saturated methyl ketones with a chain length of C_{11} to C_{15}, while blend B also contained monounsaturated methyl ketones.[88] The EC_{50} and LOEC values for blend A were 2.12 mg L^{-1} and 1.50 mg L^{-1}, respectively. The EC_{50} and LOEC values for blend B were 1.65 mg L^{-1} and 1.20 mg L^{-1}, respectively (Table 3). The aquatic toxicity of methyl ketones on fish was similar to that of WAF for gasoline and was lower than that of WAF for diesel. Regarding all examined factors that describe ecotoxicology, the methyl ketones were around ten times less toxic than diesel. Methyl ketones can be considered a less toxic fuel regarding the toxic effects on ecosystems.

Table 3 Aquatic toxicity on fish for methyl ketones, gasoline, and diesel. Methyl ketones A is a mixture of the saturated methyl ketones with 22.4 vol% 2-undecanone, 51.2 vol% 2-tridecanone, and 26.4 vol% 2-pentadecanone. Methyl ketones B is derived from cultivation broth and also contains the monounsaturated methyl ketones, namely 2-undecanone, 2-tridecanone, 2-tridecenone, 2-pentadecanone, 2-pentadecenone, and 2-heptadecenone. $LC_{50} = 50\%$ lethal concentration; EC_{50} = median effective concentration; LOEC = lowest observed adverse effect concentration; NOEC = highest concentration with no observed adverse effects; n.c.: not calculable. The data are shown as mean values with standard deviations of triplicate measurements

Values [mg L^{-1}]	Methyl ketones A	Methyl ketones B	Diesel[89]
LC_{50}	n.c.	2.01 ± 0.42	0.23
EC_{50}	2.12 ± 0.35	1.65 ± 0.20	n.c.
LOEC	1.50 ± 0.18	1.20 ± 0.39	0.22
NOEC	n.c.	1.00 ± 0.26	0.15

Conclusions

There are molecules that can be produced sustainably by using microorganisms, and other molecules that are described to have favourable cetane numbers for application in diesel engines. In this study, it was shown that with the methyl ketones, the two aspects of sustainable production and potential for real-life applications can be combined. It was demonstrated that a solvent screening and the usage of the advanced MPLR enable a bioprocess for superior production of methyl ketones from renewable sugars. An extensive investigation of the properties of the methyl ketones revealed that regarding most tested criteria, this blend is already backward-compatible with the existing vehicle fleet at the current status. The examination in a research engine showed that the methyl ketone blend enables beneficial, efficient, and clean combustion already with diesel calibration and hardware, while the benefits were especially pronounced at low loads. The blend also has a reduced ecotoxicological impact compared to currently used diesel, presumably resulting in the demonstrated shorter recommended storage times. This issue can easily be solved by using additives that can improve storability. Additionally, additives are necessary for lowering the freezing point, and some adaptions regarding sealing materials will be required. Future investigations will focus on techno-economic and environmental analyses. The applicability of alternative, potentially CO_2 or plastic-derived carbon sources for the biotechnological production of the methyl ketones will be tested.[90] Blending the methyl ketones with existing diesel might lower the entrance barrier and contribute thereby directly to CO_2 reduction, a strategy that should be investigated. Concluding, a multi-discipline approach was shown to produce, test, and evaluate a diesel fuel blend that can directly contribute to lowering the greenhouse gas emissions of the existing diesel engines.

Author contributions

Conflicts of interest

There are no conflicts to declare.

Acknowledgements

References

1 C. Dellomonaco, J. M. Clomburg, E. N. Miller and R. Gonzalez, *Nature*, 2011, **476**, 355–359.

2 EDGAR, *Distribution of Carbon Dioxide Emissions Worldwide in 2021, by Sector*, https://www.statista.com/statistics/1129656/global-share-of-co2-emissions-from-fossil-fuel-and-cement/, (accessed July 05, 2023).

3 IEA, *Net Zero by 2050*, IEA, 2021.

4 E. Çabukoglu, G. Georges, L. Küng, G. Pareschi and K. Boulouchos, *Transp. Res. Part C Emerg. Technol.*, 2018, **88**, 107–123.

5 H. Kim, K. Y. Koo and T.-H. Joung, *J. Int. Marit. Saf. Environ. Aff. Shipp.*, 2020, **4**, 26–31.

6 S. Osella, J. Kargul, M. Izzo and B. Trzaskowski, in *Theory and Simulation in Physics for Materials Applications: Cutting-Edge Techniques in Theoretical and Computational Materials Science*, ed. E. V. Levchenko, Y. J. Dappe and G. Ori, Springer International Publishing, Cham, 1st edn, 2020, pp. 227–274.

7 A. Ramirez, S. M. Sarathy and J. Gascon, *Trends Chem.*, 2020, **2**, 785–795.

8 P. Burkardt, M. Fleischmann, T. Wegmann, M. Braun, J. Knöll, L. Schumacher, F. vom Lehn, B. Lehrheuer, M. Meinke, H. Pitsch, R. Kneer, W. Schröder and S. Pischinger, in *Engines and Fuels for Future Transport*, ed. G. Kalghatgi, A. K. Agarwal, F. Leach and K. Senecal, Springer Singapore, Singapore, 1st edn, 2022, pp. 205–231.

9 M. Contestabile, G. J. Offer, R. Slade, F. Jaeger and M. Thoennes, *Energy Environ. Sci.*, 2011, **4**, 3754–3772.

10 K. Lokesh, L. Ladu and L. Summerton, *Sustainability*, 2018, **10**, 1695.

11 M. A. Masri, D. Garbe, N. Mehlmer and T. B. Brück, *Energy Environ. Sci.*, 2019, **12**, 2717–2732.

12 L. R. Lynd, G. T. Beckham, A. M. Guss, L. N. Jayakody, E. M. Karp, C. Maranas, R. L. McCormick, D. Amador-Noguez, Y. J. Bomble, B. H. Davison, C. Foster, M. E. Himmel, E. K. Holwerda, M. S. Laser, C. Y. Ng, D. G. Olson, Y. Román-Leshkov, C. T. Trinh, G. A. Tuskan, V. Upadhayay, D. R. Vardon, L. Wang and C. E. Wyman, *Energy Environ. Sci.*, 2022, **15**, 938–990.

13 T. N. Do, C. You and J. Kim, *Energy Environ. Sci.*, 2022, **15**, 169–184.

14 D. Dahiya, H. Sharma, A. K. Rai and P. S. Nigam, *AIMS Microbiol.*, 2022, **8**, 83–102.

15 J. Wesseler, G. Kleter, M. Meulenbroek and K. P. Purnhagen, *Appl. Econ. Perspect. Policy*, 2023, **45**, 839–859.

16 G. Antranikian and W. R. Streit, *Extremophiles*, 2022, **26**, 10.

17 M. Antar, D. Lyu, M. Nazari, A. Shah, X. Zhou and D. L. Smith, *Renewable Sustainable Energy Rev.*, 2021, **139**, 110691.

18 K. W. Harrison and B. G. Harvey, *Sustainable Energy Fuels*, 2018, **2**, 367–371.

19 E. B. Goh, E. E. Baidoo, J. D. Keasling and H. R. Beller, *Appl. Environ. Microbiol.*, 2012, **78**, 70–80.

20 Z. Zhu, Y. J. Zhou, A. Krivoruchko, M. Grininger, Z. K. Zhao and J. Nielsen, *Nat. Chem. Biol.*, 2017, **13**, 360–362.

21 E. K. R. Hanko, C. M. Denby, I. N. V. Sanchez, W. Lin, K. J. Ramirez, C. A. Singer, G. T. Beckham and J. D. Keasling, *Metab. Eng.*, 2018, **48**, 52–62.

22 J. Dong, Y. Chen, V. T. Benites, E. E. K. Baidoo, C. J. Petzold, H. R. Beller, A. Eudes, H. V. Scheller, P. D. Adams, A. Mukhopadhyay, B. A. Simmons and S. W. Singer, *Biotechnol. Bioeng.*, 2019, **116**, 1909–1922.

23 S. C. Nies, R. Dinger, Y. Chen, G. G. Wordofa, M. Kristensen, K. Schneider, J. Büchs, C. J. Petzold, J. D. Keasling, L. M. Blank and B. E. Ebert, *Appl. Environ. Microbiol.*, 2019, **86**, e03038.

24 S. C. Nies, T. B. Alter, S. Nölting, S. Thiery, A. N. T. Phan, N. Drummen, J. D. Keasling, L. M. Blank and B. E. Ebert, *Metab. Eng.*, 2020, **62**, 84–94.

25 J. Dafoe and A. Daugulis, *Biotechnol. Lett.*, 2014, **36**, 443–460.

26 U. A. Salas-Villalobos, R. V. Gómez-Acata, J. Castillo-Reyna and O. Aguilar, *J. Chem. Technol. Biotechnol.*, 2021, **96**, 2735–2743.

27 J. Volmer, A. Schmid and B. Buhler, *Biotechnol. J.*, 2017, **12**, 1600558.

28 M. R. Pursell, M. A. Mendes-Tatsis and D. C. Stuckey, *Biotechnol. Bioeng.*, 2004, **85**, 155–165.

29 M. Anvari, H. Pahlavanzadeh, E. Vasheghani-Farahani and G. Khayati, *J. Ind. Microbiol. Biotechnol.*, 2009, **36**, 873.

30 H. Gonzalez-Penas, T. A. Lu-Chau, M. T. Moreira and J. M. Lema, *Appl. Microbiol. Biotechnol.*, 2014, **98**, 5915–5924.

31 G. P. Prpich and A. J. Daugulis, *Biotechnol. Bioeng.*, 2007, **97**, 536–543.

32 P. Demling, M. von Campenhausen, C. Grütering, T. Tiso, A. Jupke and L. M. Blank, *Green Chem.*, 2020, **22**, 8495–8510.

33 C. Brandenbusch, S. Glonke, J. Collins, R. Hoffrogge, K. Grunwald, B. Bühler, A. Schmid and G. Sadowski, *Biotechnol. Bioeng.*, 2015, **112**, 2316–2323.

34 K. Khosravi-Darani and E. Vasheghani-Farahani, *Crit. Rev. Biotechnol.*, 2005, **25**, 231–242.

35 J. T. Boock, A. J. E. Freedman, G. A. Tompsett, S. K. Muse, A. J. Allen, L. A. Jackson, B. Castro-Dominguez, M. T. Timko, K. L. J. Prather and J. R. Thompson, *Nat. Commun.*, 2019, **10**, 587.

36 S. Glonke, G. Sadowski and C. Brandenbusch, *J. Ind. Microbiol. Biotechnol.*, 2016, **43**, 1527–1535.

37 L. Janssen, G. Sadowski and C. Brandenbusch, *Biotechnol. J.*, 2023, **18**, e2200489.

38 M. von Campenhausen, P. Demling, P. Bongartz, A. Scheele, T. Tiso, M. Wessling, L. M. Blank and A. Jupke, *Discover Chem. Eng.*, 2023, **3**, 2.

39 *Germany Pat.*, WO2017149099A1, 2017.

40 B. Weber, M. von Campenhausen, T. Maßmann, A. Bednarz and A. Jupke, *Chem. Eng. Sci.: X*, 2019, **2**, 100010.

41 A. Bednarz, PhD thesis, RWTH Aachen, 2019.

42 S. Hartmans, J. P. Smits, M. J. van der Werf, F. Volkering and J. A. de Bont, *Appl. Environ. Microbiol.*, 1989, **55**, 2850–2855.

43 *National Institutes of Health, PubChem*, https://pubchem.ncbi.nlm.nih.gov/, (accessed September 17, 2023).

44 *Deutsche Gesetzliche Unfallversicherung, GESTIS-Stoffdatenbank*, https://www.dguv.de/ifa/stoffdatenbank/, (accessed September 28, 2023).

45 A. Biselli, A.-L. Willenbrink, M. Leipnitz and A. Jupke, *Sep. Purif. Technol.*, 2020, **250**, 117031.

46 *Messung der kinematischen Viskosität mit dem Ubbelohde-Viskosimeter, Report DIN 51562-1*, Beuth Verlag GmbH, Berlin, 1976.

47 M. Hofmeister, A. Frische, M. Grunewald, M. A. Reddemann, C. Grütering, L. M. Blank, R. Kneer and K. Schmitz, presented in part at the 21, *International Sealing Conference*, Stuttgart, Germany, October 12-13, 2022.

48 *Grenzflächenaktive Stoffe – Bestimmung der Oberflächenspannung, Report DIN EN 14370:2004-11*, Beuth Verlag GmbH, Berlin, 2004.

49 *Elastomere Oder Thermoplastische Elastomere, Report DIN ISO 1817*, Beuth Verlag GmbH, Berlin, 2016.

50 *Dieselkraftstoff – Bestimmung der Schmierfähigkeit unter Verwendung eines Schwingungsverschleiß-Prüfgerätes (HFRR), Report DIN EN ISO 12156*, Beuth Verlag GmbH, Berlin, 2019.

51 *Elastomere Oder Thermoplastische Elastomere, Report DIN ISO 48*, Beuth Verlag GmbH, Berlin, 2016.

52 A. Klamt, F. Eckert and W. Arlt, *Annu. Rev. Chem. Biomol. Eng.*, 2010, **1**, 101–122.

53 J. Reinisch and A. Klamt, *Ind. Eng. Chem. Res.*, 2015, **54**, 12974–12980.

54 A. Schäfer, C. Huber and R. Ahlrichs, *J. Chem. Phys.*, 1994, **100**, 5829–5835.

55 A. D. Becke, *Phys. Rev. A*, 1988, **38**, 3098–3100.

56 J. P. Perdew, *Phys. Rev. B: Condens. Matter Mater. Phys.*, 1986, **33**, 8822–8824.

57 P. Seidenspinner, *AFIDA 2805 Advanced Fuel Ignition Delay Analyzer Research Versions*, ASG Analytik-Service AG, Neusaeess, Germany, 2023.

58 D02 Comittee, *Standard Test Method for Determination of Indicated Cetane Number (ICN) of Diesel Fuel Oils Using a Constant Volume Combustion Chamber Reference Fuels Calibration Method, Report ASTM D8183-22*, 2022.

59 A. Janssen, M. Muether, S. Pischinger, A. Kolbeck and M. Lamping, *Tailor-Made Fuels: The Potential of Oxygen Content in Fuels for Advanced Diesel Combustion Systems, Report 2009-01-2765*, SAE Technical Paper Series, 2009.

60 B. Heuser, F. Kremer, S. Pischinger, J. Julis and W. Leitner, *Optimization of Diesel Combustion and Emissions with Newly Derived Biogenic Alcohols, Report 0148-7191*, SAE International, 2013.

61 B. Heuser, M. Jakob, T. Laible, F. Kremer and S. Pischinger, C_8-Oxygenates for Clean Diesel Combustion, Report 2014-01-1253, 2014.

62 C. Honecker, B. Lehrheuer, S. Pischinger and K. A. Heufer, *Fuel*, 2023, **345**, 128184.

63 B. Leuchtle, L. Epping, W. Xie, S. J. Eiden, W. Koch, D. Diarra, K. Lucka, M. Zimmermann and L. M. Blank, *Int. Biodeterior. Biodegrad.*, 2018, **132**, 84–93.

64 P. Ackermann, K. E. Braun, P. Burkardt, S. Heger, A. Konig, P. Morsch, B. Lehrheuer, M. Surger, S. Volker, L. M. Blank, M. Du, K. A. Heufer, M. Ross-Nickoll, J. Viell, N. von der Assen, A. Mitsos, S. Pischinger and M. Dahmen, *ChemSusChem*, 2021, **14**, 5254–5264.

65 S. Heger, J. Brendt, H. Hollert, M. Roß-Nickoll and M. Du, *Sci. Total Environ.*, 2021, **764**, 142902.

66 A. Inoue and K. Horikoshi, *J. Ferment. Bioeng.*, 1991, **71**, 194–196.

67 H. J. Heipieper, F. J. Weber, J. Sikkema, H. Keweloh and J. A. M. de Bont, *Trends Biotechnol.*, 1994, **12**, 409–415.

68 D. Prat, A. Wells, J. Hayler, H. Sneddon, C. R. McElroy, S. Abou-Shehada and P. J. Dunn, *Green Chem.*, 2016, **18**, 288–296.

69 M. F. Hassan, M. Z. M. Saman, S. Sharif and B. Omar, *Clean Technol. Environ. Policy*, 2016, **18**, 63–79.

70 S. P.-D. L. Cuesta, L. Knopper, L. A. M. van der Wielen and M. C. Cuellar, *Biofuels, Bioprod. Biorefin.*, 2019, **13**, 140–152.

71 S. Pedraza-de la Cuesta, L. Keijzers, L. A. M. van der Wielen and M. C. Cuellar, *Biotechnol. J.*, 2018, **13**, e1700478.

72 E. B. Goh, E. E. K. Baidoo, H. Burd, T. S. Lee, J. D. Keasling and H. R. Beller, *Metab. Eng.*, 2014, **26**, 67–76.

73 E. B. Goh, Y. Chen, C. J. Petzold, J. D. Keasling and H. R. Beller, *Biotechnol. Bioeng.*, 2018, **115**, 1161–1172.

74 S. C. Nies, T. B. Alter, S. Nölting, S. Thiery, A. N. T. Phan, N. Drummen, J. D. Keasling, L. M. Blank and B. E. Ebert, *Metab. Eng.*, 2020, **62**, 84–94.

75 J. Meyers, J. B. Mensah, F. J. Holzhäuser, A. Omari, C. C. Blesken, T. Tiso, S. Palkovits, L. M. Blank, S. Pischinger and R. Palkovits, *Energy Environ. Sci.*, 2019, **12**, 2406–2411.

76 A. Nicolau, C. V. Lutckmeier, D. Samios, M. Gutterres and C. M. S. Piatnick, *Fuel*, 2014, **117**, 26–32.

77 B. Graziano, F. Kremer, S. Pischinger, K. A. Heufer and H. Rohs, *SAE Int. J. Fuels Lubr.*, 2015, **8**, 62–79.

78 M. Zubel, O. P. Bhardwaj, B. Heuser, B. Holderbaum, S. Doerr and J. Nuottimäki, *SAE Int. J. Fuels Lubr.*, 2016, **9**, 481–492.

79 O. P. K. Bhardwaj, F. Andreas, T. Kkoerfer and M. Honkanen, *SAE Int. J. Fuels Lubr.*, 2013, **6**, 157–169.

80 M. J. Surger and L. M. Blank, *Eng. Life Sci.*, 2022, **22**, 508–518.

81 P. Suppajariyawat, A. F. B. d. Andrade, M. Elie, M. Baron and J. Gonzalez-Rodriguez, *Open Chem.*, 2019, **17**, 183–197.

82 M. Gürü, U. Karakaya, D. Altıparmak and A. Alıcılar, *Energy Convers. Manage.*, 2002, **43**, 1021–1025.

83 N. Graf and J. Altenbuchner, *Appl. Microbiol. Biotechnol.*, 2013, **97**, 8239–8251.

84 J. Frey, S. Kaßner and B. Schink, *Curr. Microbiol.*, 2021, **78**, 1763–1770.

85 A. Völker, A. Kirschner, U. T. Bornscheuer and J. Altenbuchner, *Appl. Microbiol. Biotechnol.*, 2008, **77**, 1251–1260.

86 F. E. Khalid, Z. S. Lim, S. Sabri, C. Gomez-Fuentes, A. Zulkharnain and S. A. Ahmad, *J. Mar. Sci. Eng.*, 2021, **9**, 155.

87 L. N. Komariah, S. Arita, M. Rendana, C. Ramayanti, N. L. Suriani and D. Erisna, *Heliyon*, 2022, **8**, e09264.

88 M. Froning, C. Grütering, L. M. Blank and H. Hayen, *Rapid Commun. Mass Spectrom.*, 2023, **37**, e9457.

89 C. Eickhoff, W. Hobbs, J. Weakland, A. Buchan, K. Lee, M. Tran and H. C. Bailey, *Presented in Part at the Salis Sea Ecosystem Conference, April 21*, 2020.

90 L. M. Blank, T. Narancic, J. Mampel, T. Tiso and K. O'Connor, *Curr. Opin. Biotechnol.*, 2020, **62**, 212–219.